NUWC-NPT Technical Report 10,534
30 November 1995

Current Pulsing: A Method to Reduce the Production of Magnetohydrodynamic Electrode Bubbles

S. A. Huyer
Weapons Technology and Undersea Systems Department

Naval Undersea Warfare Center Division
Newport, Rhode Island

DISCLAIMER NOTICE

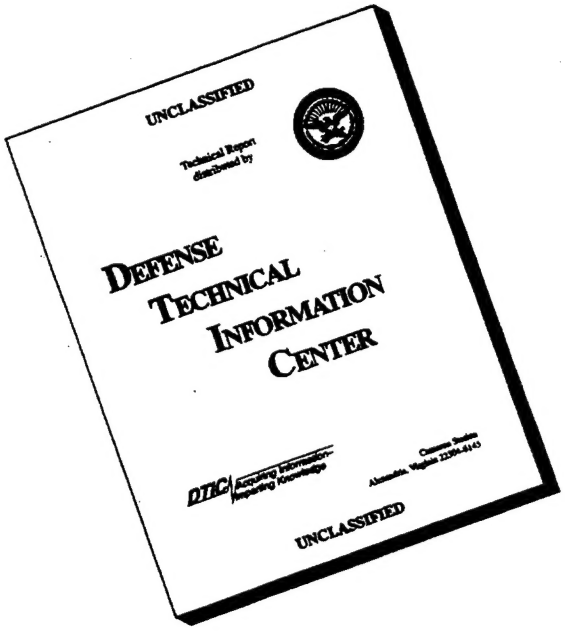

THIS DOCUMENT IS BEST QUALITY AVAILABLE. THE COPY FURNISHED TO DTIC CONTAINED A SIGNIFICANT NUMBER OF PAGES WHICH DO NOT REPRODUCE LEGIBLY.

PREFACE

This work was conducted as part of the Naval Undersea Warfare Center Division Newport Bid and Proposal Program, principal investigator S. A. Huyer (Code 8233).

The technical reviewer for this report was P. Hendricks (Code 8231).

The author appreciates J. Mulherin for his assistance in setting up the experiment; J. Papp for her helpful comments regarding the electrochemistry; and P. Hendricks for his thorough review and comments.

Reviewed and Approved: 30 November 1995

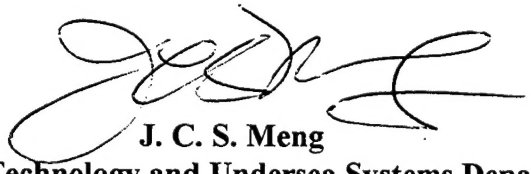

J. C. S. Meng
Head, Weapons Technology and Undersea Systems Department

REPORT DOCUMENTATION PAGE

Form Approved
OMB No. 0704-0188

1. AGENCY USE ONLY *(Leave blank)*	2. REPORT DATE	3. REPORT TYPE AND DATES COVERED
	30 November 1995	

4. TITLE AND SUBTITLE
Current Pulsing: A Method to Reduce the Production of Magnetohydrodynamic Electrode Bubbles

5. FUNDING NUMBERS

6. AUTHOR(S)

S. A. Huyer

7. PERFORMING ORGANIZATION NAME(S) AND ADDRESS(ES)

Naval Undersea Warfare Center Division
1176 Howell Street
Newport. RI 02841-1708

8. PERFORMING ORGANIZATION REPORT NUMBER
TR 10,534

9. SPONSORING/MONITORING AGENCY NAME(S) AND ADDRESS(ES)

10. SPONSORING/MONITORING AGENCY REPORT NUMBER

11. SUPPLEMENTARY NOTES

12a. DISTRIBUTION/AVAILABILITY STATEMENT

Cleared for public release by competent authority.

12b. DISTRIBUTION CODE

13. ABSTRACT *(Maximum 200 words)*

Significant bubble production results during magnetohydrodynamic (MHD) applications in a conducting fluid. Bubbles, caused by the presence of an electrical field, create severe difficulties in collecting and analyzing reliable test data. Two of the most widely accepted flow measurement techniques, hot-film and laser Doppler velocimetry, have problems in sea water MHD flows. This report discusses some experiments conducted to understand the bubble production process more clearly and to quantify the formation of bubbles on MHD electrodes. Cyclical square-wave pulsing of the electrodes at differing frequencies and duty cycles was accomplished using a controller. Four different solutions of differing compositions and conductivity were examined to gauge this effect. To quantify the bubble-production processes, a closeup video camera that provided 150x magnification was used. A threshold voltage was then defined as the point at which gas bubbles were observed on the electrode surface. Threshold voltage was then examined as a function of time for the four conducting solutions examined. Finally, actual effects of bubble formation over operating hot-film probes were visually examined to demonstrate the effects of the bubble production on hot-film performance.

14. SUBJECT TERMS

Electrolysis Electromagnetic Fields Lorentz Force
Magnetohydrodynamics (MHD) MHD Flows

15. NUMBER OF PAGES
30

16. PRICE CODE

17. SECURITY CLASSIFICATION OF REPORT	18. SECURITY CLASSIFICATION OF THIS PAGE	19. SECURITY CLASSIFICATION OF ABSTRACT	20. LIMITATION OF ABSTRACT
Unclassified	Unclassified	Unclassified	SAR

TABLE OF CONTENTS

LIST OF ILLUSTATIONS

LIST OF TABLES

LIST OF ABBREVIATIONS AND SYMBOLS

DSA	Dimensionally stable anode
H_2O	Water
MDTI	McDonnell Douglas Technologies Incorporated
MHD	Magnetohydrodynamic
$MgSO_4$	Magnesium sulfur oxide
NaCl	Sodium chloride
NaOH	Sodium hydroxide
VHS	Very high speed
V_{thresh}	Bubble-formation threshold voltage

CURRENT PULSING: A METHOD TO REDUCE THE PRODUCTION OF MHD ELECTRODE BUBBLES

1. INTRODUCTION

Using magnetohydrodynamics (MHD) to control flow for undersea vehicles that operate in an electrically conducting medium has shown great potential (Henoch and Stace (1995), Meng, (1995)). When an electric field and a magnetic field interact, a Lorentz force is produced. The magnitude and direction of the force is proportional to the cross product of the current and magnetic field. If a magnetic field is appropriately produced and the current passes through a conducting fluid medium, such as salt water, a body force acts on the fluid itself. This physical phenomenon has the potential to control the flow. Nosenchuck and Brown (1995) proposed methods to use MHD to control boundary-layer turbulence, thus reducing the drag on a moving vehicle. Henoch (1992) and Henoch et al. (1995) have reported some quantitative and qualitative data regarding the effects of MHD forces on a turbulent-boundary layer. Meng (1995) proposed a control system methodology that utilizes MHD to manipulate the flow in a turbulent boundary and thus reduce drag.

Much of the debate that continues on using MHD to reduce turbulent drag can be attributed to the problems of collecting and analyzing reliable test data. Two of the most widely accepted flow measurement techniques, hot-film and laser Doppler velocimetry, have problems in sea water MHD flows. These problems stem from the undesired production of bubbles at the MHD electrodes. Standard hot-film probes encounter difficulties with bubble formation on the surface of the hot-film, especially in the wake of the bubble-producing anode and cathode elements. In laser Doppler velocimetry, the bubbles act as seed particles, thus producing erroneous results. These bubble formations, which consist of gases, have substantially different heat-transfer characteristics than a liquid (sea water). Because the probes are no longer in direct contact with the sea water, they cannot measure the proper heat transfer and the resulting velocity fluctuations in the flow. Diminished velocity fluctuations could be mistaken for turbulent drag reduction.

Bubbles are formed on the electrodes because of electrolysis. The primary chemical components of sea water are water (H_2O) and salts, predominantly sodium chloride (NaCl). The water breaks the electrostatic bonds, causing the salts to ionize thus making the fluid electrically conductive. When an electric current passes through the salt water, a chemical reaction occurs (Hildebrand and Powell, 1952). At the cathode (negative terminal), electrons enter the water resulting in a chemical reaction that causes disassociation of the water molecule to produce hydrogen gas. At the anode (positive terminal), electrons leave the conducting medium resulting in a chemical reaction that produces chlorine. Previous research conducted at Princeton University by Nosenchuck (1995) suggests that pulsing the current to the electrodes in the form of a square wave with reversing polarity delayed bubble formation to higher voltages. The purpose of the pulsing, however, was to control the Lorentz force. Reduced bubble production was a desirable consequence. Physically, bubble production is thought to be delayed because a finite time is required to disassociate the molecules into gaseous form and accumulate sufficient

mass to form gas bubbles. The extent to which pulsing is effective in terms of controlling and reducing bubble production has not been quantified.

This report summarizes experiments conducted to quantify the formation of bubbles on MHD electrodes. Cyclical square-wave pulsing of the electrodes at differing frequencies and duty cycles was accomplished using a controller. Four different solutions of differing compositions and conductivity were examined to gauge this effect. To quantify the bubble-production processes, a closeup video camera that provided 150x magnification was used. A threshold voltage was then defined as the point at which gas bubbles were observed on the electrode surface. Threshold voltage was then examined as a function of time for the four conducting solutions examined. Finally, actual effects of bubble formation over operating hot-film probes were visually examined to demonstrate the effects of the bubble production on hot-film performance.

2. EXPERIMENTAL METHODS

A 40-gallon aquarium (figure 1) was filled with 100 liters of tap water. Table salt (100-percent NaCl) was added to produce two saline solutions of 1.5 percent and 3.5 percent. In addition, a 0.4-percent sodium hydroxide (NaOH) solution was prepared. NaOH was examined because MHD experiments conducted by McDonnell Douglas Technologies Incorporated (MDTI) used 0.4-percent NaOH as the conducting fluid. The NaOH also provided an additional conducting fluid with which to compare. To provide a basis for comparative results, bubble experiments were conducted in sea water. The sea water was taken from Narragansett Bay and was found to have a total solids of 0.03319 g/ml. Conductivity levels for each solution were tested, the results of which are listed in table 1. The conductivity was measured with a YSI Model 35 conductance meter calibrated with a 100,000-microsiemens/cm conductivity standard and is reported to ± 0.1 millimho. As can be seen, the 3.5-percent NaCl solution had the highest conductivity. The 1.5-percent NaCl solution and 0.4-percent NaOH solution have roughly equivalent conductivities. The sea water conductivity is approximately 20 percent less than the 3.5-percent NaCl solution.

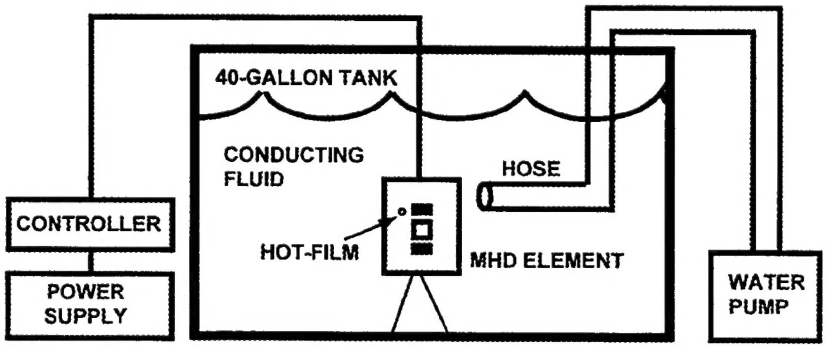

Figure 1a. Experimental Setup

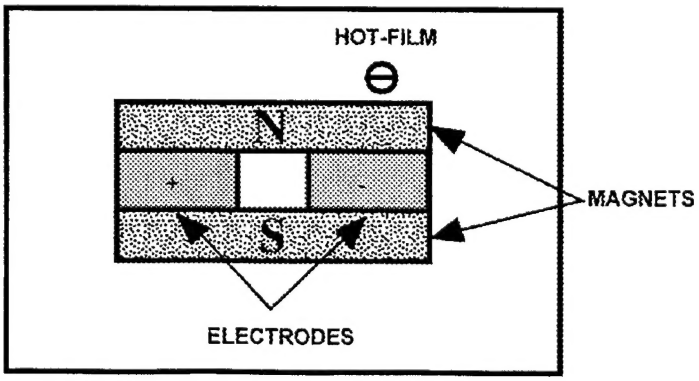

Figure 1b. MHD Element

Table 1. Conductivity Levels for Various Solutions

Conducting Fluid	Conductivity (millimho)	Temperature (°C)
Sea water	42.4	22.32
0.4% NaOH	18.6	22.25
1.5% NaCl	24.97	22.20
3.5% NaCl	50.8	21.86

A single MHD element consisting of two magnets and two electrodes (figure 1(b)) was then placed in the aquarium and was held in place by a stainless steel support. Because the support was electrically conductive, a thin layer of plastic was used to insulate the support from the MHD element. The MHD element was constructed on a 10.8-cm x 12.7-cm x 3.2-mm thick plastic base. Two strip magnets were placed along the entire length of the plastic base with one strip aligned north and the other south. The electrodes were constructed of 2.86-cm x 1.27-cm x 1.6-mm thick dimensionally stable anodes (DSA). The DSAs were made of titanium and coated with a rare-earth oxide to prevent corrosion. The electrodes were then placed between the two magnet strips. The anode and cathode were separated by a 1.27-cm^2 piece of plastic.

Investigation of bubble formation was conducted for both steady and pulsing test cases. A 1000-W Hewlett Packard power supply was used to provide voltage to the MHD element. The power supply was connected to a controller, which converted the constant voltage into a bipolar square wave. It was possible to adjust the frequency of the square wave from 2 Hz to 500 Hz and adjust the duty cycle from 25 percent to 50 percent. Duty cycle was defined as the time of positive voltage relative to the entire period. For a standard bipolar square wave, therefore, duty cycle is 50 percent because 50 percent of the time the voltage is positive and 50 percent of the time, it is negative. For duty cycles less than 50 percent, there will be times when there is zero-voltage. The time of zero-voltage will be 50 percent minus the duty cycle. Therefore, for a square wave where the voltage is 25 percent positive, 25 percent off, 25 percent negative, and 25 percent off, the duty cycle is 25 percent. Square wave signals for 25-percent and 50-percent duty cycles were used to provide the voltage variations in the current experiments. These square waves are shown in figure 2.

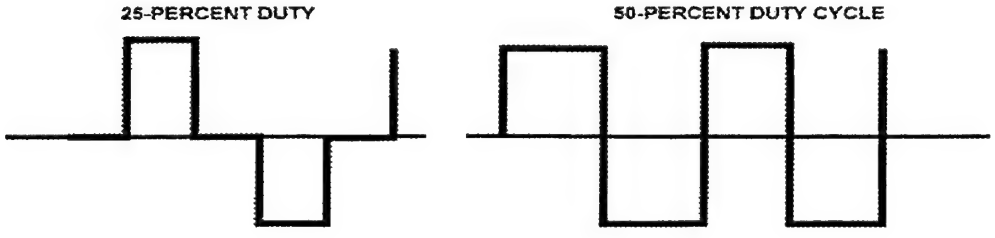

Figure 2. Square-Wave Signals for 25-Percent and 50-Percent Duty Cycle

Results of bubble formation on the surface of the MHD electrode were documented using a standard very high speed (VHS) video camera/recorder. Closeup views (150x magnification) of the upper electrode (negatively charged for positive input signal) were studied for evidence of initial bubble production. At a certain voltage, bubbles formed directly and were carried upward by the buoyancy effects; that point was defined as the bubble-initiation voltage. Initial experiments showed that the point where the anode is closest to the cathode is the region of greatest bubble production. This observation is consistent with calculations showing that the strongest electrical fields are found at this point. Several tests were conducted for sea water for the steady state case to approximate the inherent error in judging the threshold voltage. For 10 tests, data were found to be consistent to within 5 percent of the actual voltage. Therefore, the experimental error in determining the bubble threshold voltage was approximated at 5 percent of the measured voltage.

After the examination of bubble production by the MHD element was completed, the effects of bubble production on a single element, hot-film probe was investigated. A 1/8-inch pilot hole was drilled just above the MHD element to attach the hot-film probe (model 1237-W, constructed of 1/8-inch diameter stainless steel, manufactured by TSI Inc.). A thin plastic tube was then inserted and wires leading to each side of the film attached. The film itself was made of 1.02-mm x 0.17-mm platinum and coated with quartz crystal to electrically insulate it from the conducting fluid. The MHD element was located proximal to the hot-film and operated at 5.0-V steady-state potential, which was found to produce a sufficiently dense bubble stream that could advect over the hot-film probe. A pump/hose attachment was used to generate a localized velocity field. Figure 3 shows pictures of the three different pump positions that were used.

In position 1 (figure 3(a)), the hose was placed to provide a local cross-flow velocity that was normal to the bubble stream over the hot-film probe. Significant bubble production was seen at both electrodes, with the thickest concentration of bubbles coming off the cathode. These bubbles were hydrogen bubbles and appear to have a bubble density larger than that of chlorine gas. The bubbles then advected upward because of the buoyancy effects and were then deflected by the cross-flow. With no flow, buoyancy effects caused the bubbles produced by the MHD element to advect directly over the hot-film probe. In position 2 (figure 3(b)), the cross-flow jet was placed immediately below the hot-film probe causing the bubble stream to be deflected away from the hot-film probe; no bubbles were allowed to advect over the hot-film probe. This position was used to isolate the probe from the bubble stream. Any effects produced by the electromagnetic fields remained. In position 3 (figure 3(c)), the hose was placed upstream of the MHD element causing the hydrogen bubble stream to advect over the probe. This position was used to more closely simulate actual experimental conditions. These bubbles were difficult to see because of their smaller size. The presence of the jet appeared to cause the bubbles to break up and form smaller bubbles. Buoyancy effects caused the bubbles to rise slightly, but a steady stream of bubbles was still advected over the hot-film.

The velocities of the bubbles could be increased as they advected over the hot-film probe. In all three cases, pump settings of 0, 20, 25, and 30 were used corresponding to flow velocities on the order of 0, 0.5, 2, and 4 ft/sec. Results of bubble formation on the probe were documented using a standard VHS video camera/recorder. Hot-film signals were noted, but not collected.

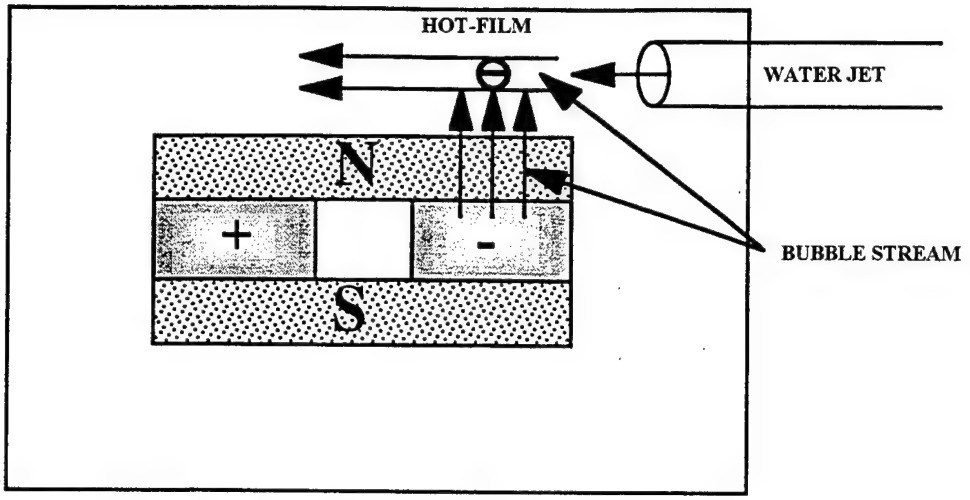

Figure 3a. Pump Position 1

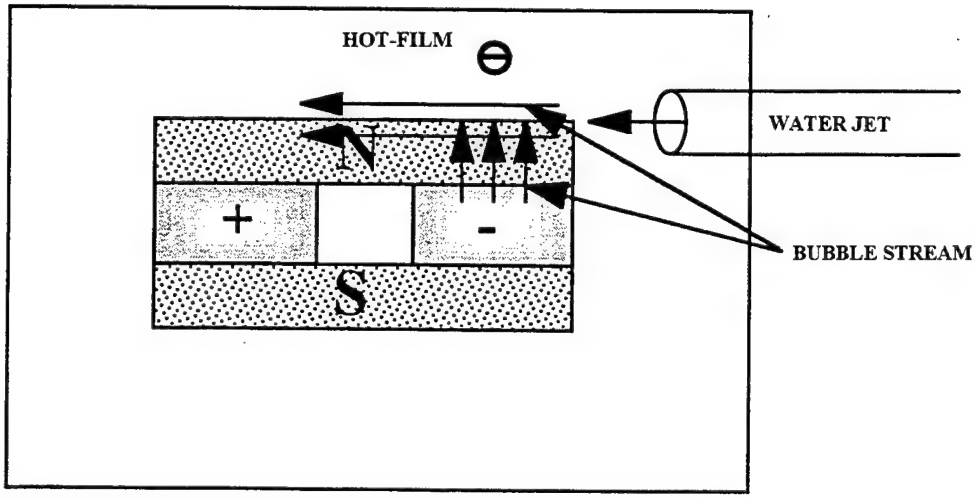

Figure 3b. Pump Position 2

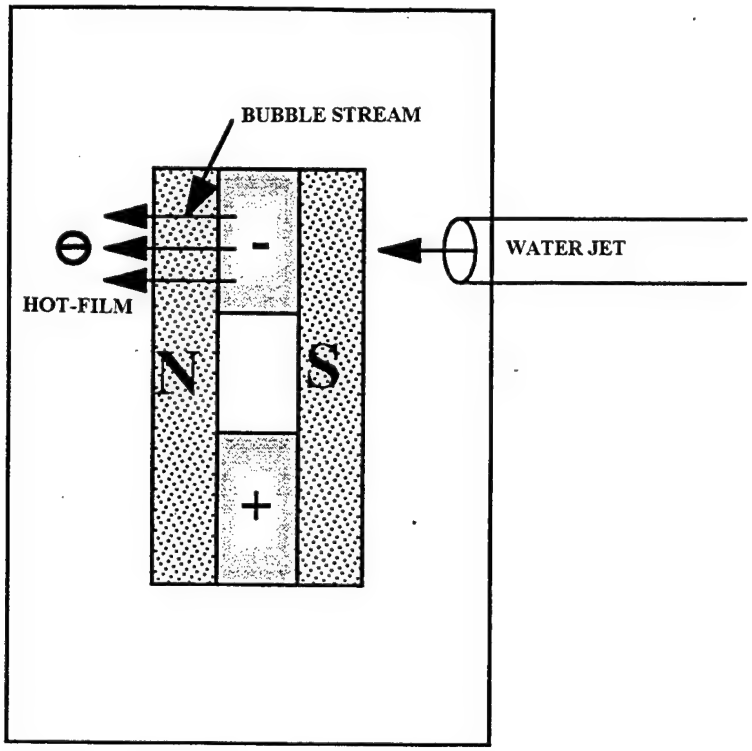

Figure 3c. Pump Position 3

3. RESULTS

3.1 BUBBLE FORMATION

To determine the bubble-formation threshold voltages (V_{thresh}) for both static and pulsing electric current through the MHD element, a qualitative examination of videos was conducted. V_{thresh} was previously defined in terms of bubble initiation of the MHD element. Table 2 shows the bubble-threshold voltages for steady-state current for the four electrically conducting fluids examined. As can be seen, steady state threshold voltage is roughly equivalent for the 1.5-percent and 3.5-percent NaCl solution and the sea water. The threshold voltage was noticeably lower for the 0.4-percent NaOH solution (1.97 V) even though the fluid conductivity was lower. To demonstrate a relative scale, all pulsed V_{thresh} data were normalized by the steady-state value of threshold voltage for sea water (2.34 V).

Table 2. Bubble-Threshold Voltages for Steady-State Current

Conducting Fluid	V_{thresh} (Volts)
Sea water	2.34
0.4% NaOH	1.97
1.5% NaCl	2.40
3.5% NaCl	2.20

Figure 4 shows bubble-threshold voltage plotted as a function of pulsing frequency for a 25-percent and 50-percent duty cycle. In general, two trends can be seen: (1) threshold voltage is significantly less for the 50-percent duty cycle than it is for the 25-percent duty cycle (this threshold voltage,however, is not exactly half) and (2) bubble-threshold voltage appears to increase logarithmically with frequency,which can be demonstrated by plotting the data in log fashion (figure 5) where a definite linear relationship between V_{thresh} and pulsing frequency appears.

Figure 6 shows bubble-threshold voltages for the 1.5-percent NaCl solution test case. Data are plotted in normal fashion to demonstrate diminished V_{thresh} for the 50-percent duty cycle and the logarithmic relationship between V_{thresh} and pulsing frequency. The data appear much less "smooth" compared with data for sea water. For the 25-percent duty cycle case, small peaks in the data appear at 32 Hz and 166 Hz; for the 50-percent duty cycle case, they appear at 100 Hz. These "jumps" in the data could be related to the overall experimental error and the fact that a qualitative basis was used to estimate the bubble-threshold voltage.

Figure 7 shows the data for the 3.5-percent NaCl test case in which there is not as great a difference in the threshold voltages between the 25-percent and 50-percent duty cycles. At

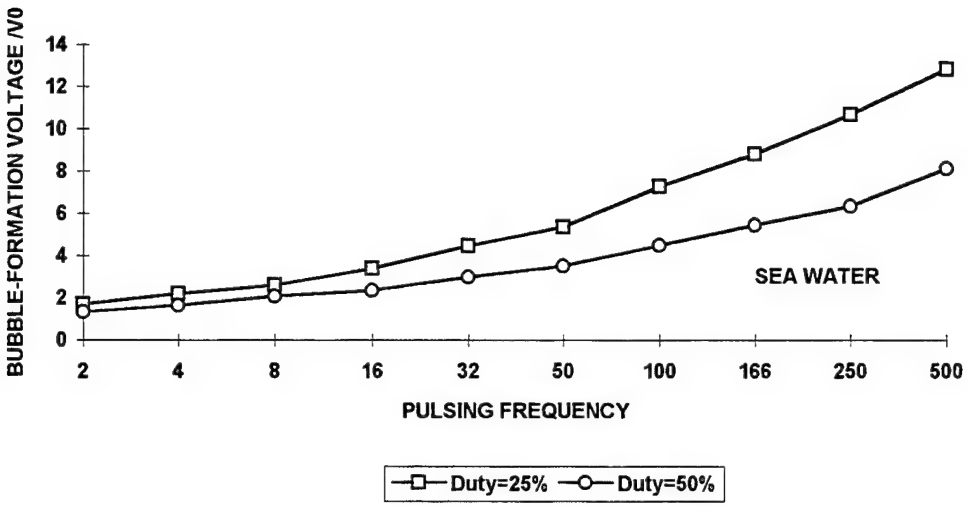

Figure 4. Sea Water Test Case: Delayed Bubble Formation Attributed to MHD Pulsing (Plotted as a Function of Pulsing Frequency)

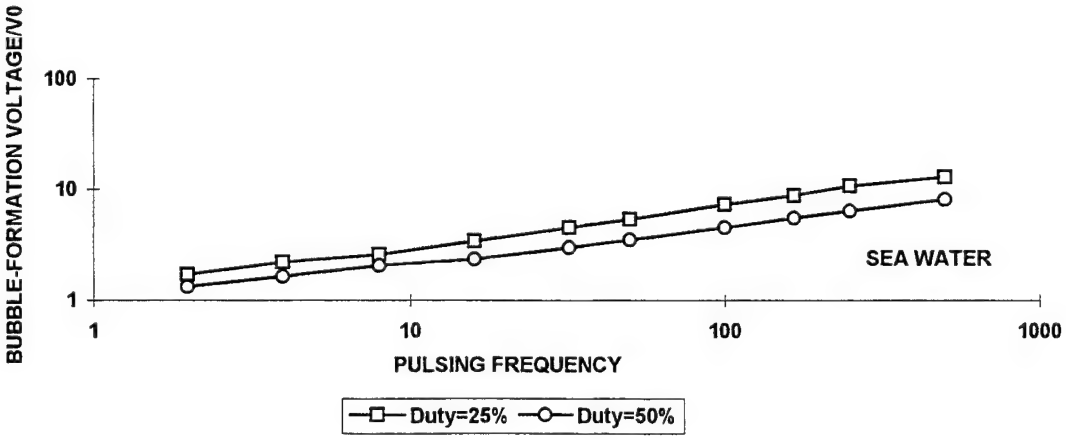

Figure 5. Sea Water Test Case: Delayed Bubble Formation Attributed to MHD Pulsing (Plotted on a Logarithmic Scale)

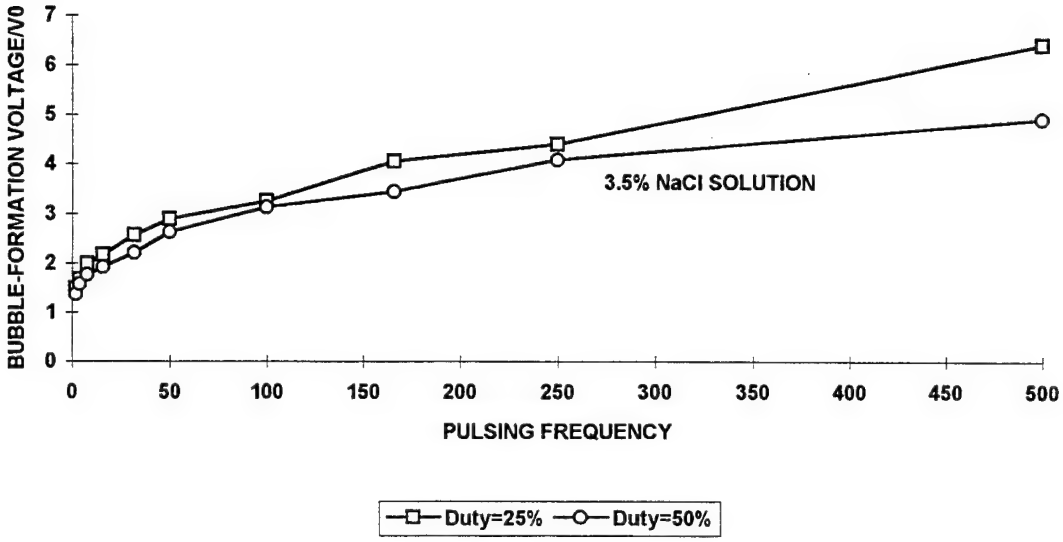

Figure 6. 1.5-Percent NaCl Solution Test Case: Delayed Bubble Formation Attributed to MHD Pulsing (Plotted as a Function of Pulsing Frequency)

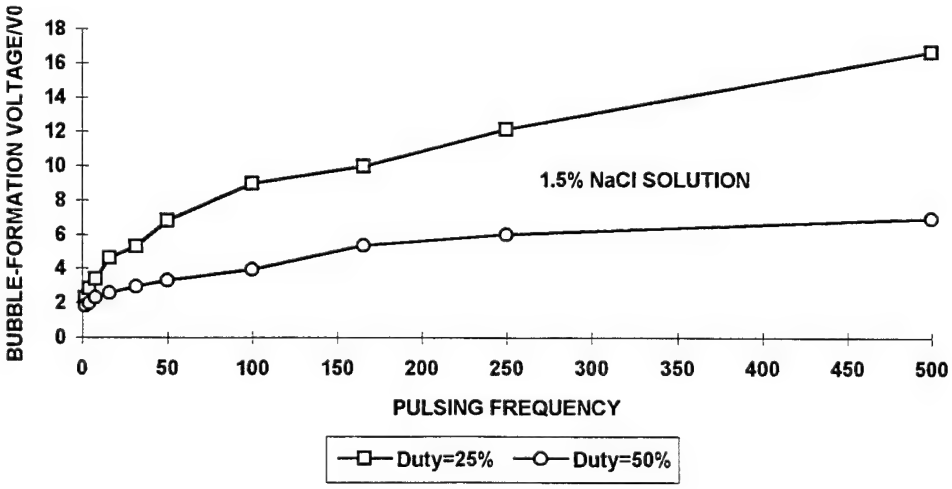

Figure 7. 3.5-Percent NaCl Solution Test Case: Delayed Bubble Formation Attributed to MHD Pulsing (Plotted as a Function of Pulsing Frequency)

500 Hz, the difference is only 1.5. Although the relationship between V_{thresh} and pulsing frequency appears logarithmic, the threshold voltages are significantly less compared with the other test cases.

Figure 8 shows the data for the 0.4-percent NaOH test case. Threshold voltages appear less for the 50-percent duty cycle than they do for the 25-percent duty cycle. The magnitude of these differences appears less compared with the sea water and 1.5-percent NaCl cases. At 500 Hz, the difference in V_{thresh} between 25-percent and 50-percent duty cycle is 4.7 and 9.7 for sea water and 1.5-percent NaCl respectively. For 0.4-percent NaOH, the difference is only 3.2. Below 50 Hz, there still appears to be a logarithmic relationship between V_{thresh} and pulsing frequency. For the higher frequencies, the relationship appears to be linear although that appearance could be the result of experimental error.

To provide comparisons between the data, figure 9 shows bubble formation voltage as a function of pulsing frequency for the 25-percent duty cycle test case. Specific test cases from MHD flat-plate experiments are plotted to provide a reference. These reference data collected by MDTI were plotted to demonstrate actual tests conducted and to show whether these test cases might generate bubbles. As wll be shown later, bubble production has significant effects on hot-film performance. Possible bubble production must, therefore, be considered when interpreting MDTI's test results. As shown in figure 9, the threshold voltage for the 3.5-percent NaCl test case is considerably lower than that for the other tests. Threshold voltage values for frequencies above 50 Hz are approximately one-half compared with the other tests cases. The sea water, 1.5-percent NaCl and NaOH cases seem roughly equivalent. At frequencies below 100 Hz, V_{thresh} for the 1.5-percent NaCl solution is consistently higher than the V_{thresh} for the NaOH and sea water solutions, which are indistinguishable. From 166 Hz to 500 Hz, V_{thresh} for the 1.5-percent NaCl solution remains highest. V_{thresh} for the sea water diminishes, so it is approximately 20 percent less at 500 Hz compared with the NaOH solution.

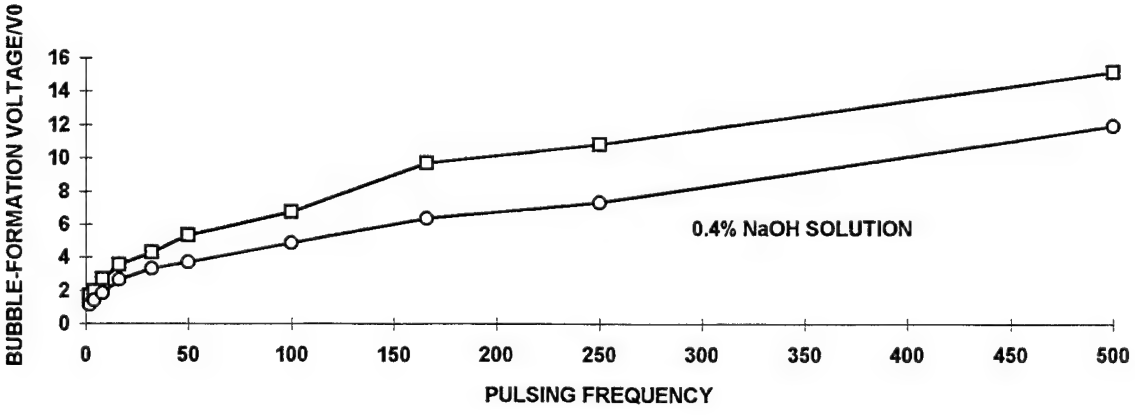

Figure 8. 0.4-Percent NaOH Solution Test Case: Delayed Bubble Formation Attributed to MHD Pulsing (Plotted as a Function of Pulsing Frequency)

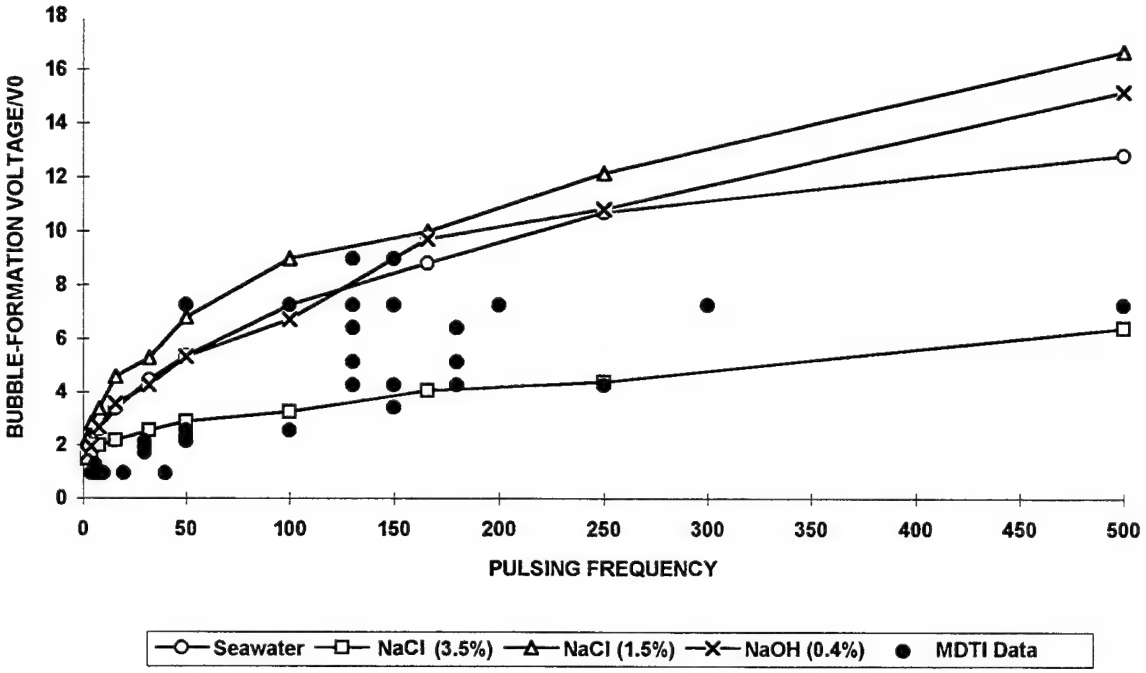

Figure 9. Relative Bubble-Threshold Voltage as a Function of Pulsing Frequency at 25-Percent Duty Cycle

Figure 10 shows bubble-formation voltages for the 50-percent duty cycle test case. The 3.5-percent NaCl solution again demonstrated the lowest threshold voltages. The threshold voltages in the sea water case appear to be consistently halfway between those in the 3.5-percent NaCl, the 1.5-percent NaCl, and the 0.4-percent NaOH test cases. V_{thresh} for the 3.5-percent NaCl solution are again considerably less compared with the other solutions. Threshold voltages for the 1.5-percent NaCl and 0.4-percent NaOH test cases are largest, with the threshold voltages for the 1.5-percent NaCl solution consistently 10 percent greater than those of the NaOH solution.

The ratio between the threshold voltages between 50-percent relative to 25-percent duty cycle is plotted in figure 11 as a function of pulsing frequency for the four conducting fluids that were examined. The ratios for the sea water are initially between 0.75 and 0.8 and then decrease to values between 0.6 and 0.7 as pulsing frequency is increased. The ratios for 3.5-percent NaCl solution remain considerably higher with values fluctuating between 0.85 and 0.95 across all pulsing frequencies. Only at 500 Hz does the ratio decrease below 0.8. Conversely, the ratios for the 1.5-percent NaCl solution are initially at 0.8, but decrease rapidly to values around 0.5. At f = 500 Hz, the ratio decreases to 0.4. The ratios for the NaOH solution are initially 0.66. As frequency increases, the ratio increases to 0.77 at 32 Hz and then drops off to 0.678 at 250 Hz. At 500 Hz, the ratio increases to 0.8.

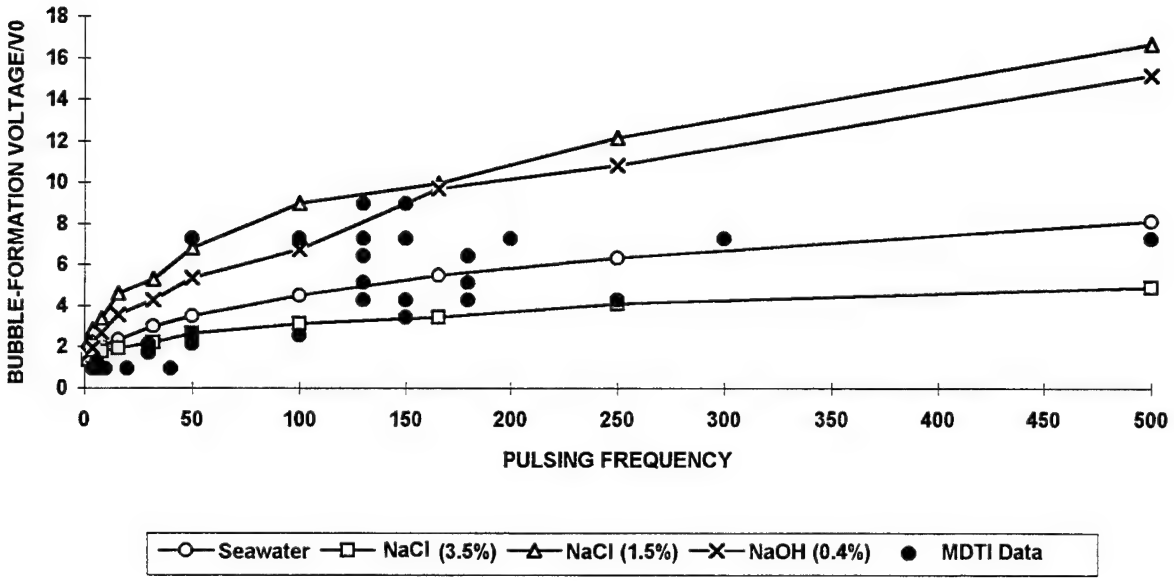

Figure 10. Relative Bubble-Threshold Voltage as a Function of Pulsing Frequency at 50-Percent Duty Cycle

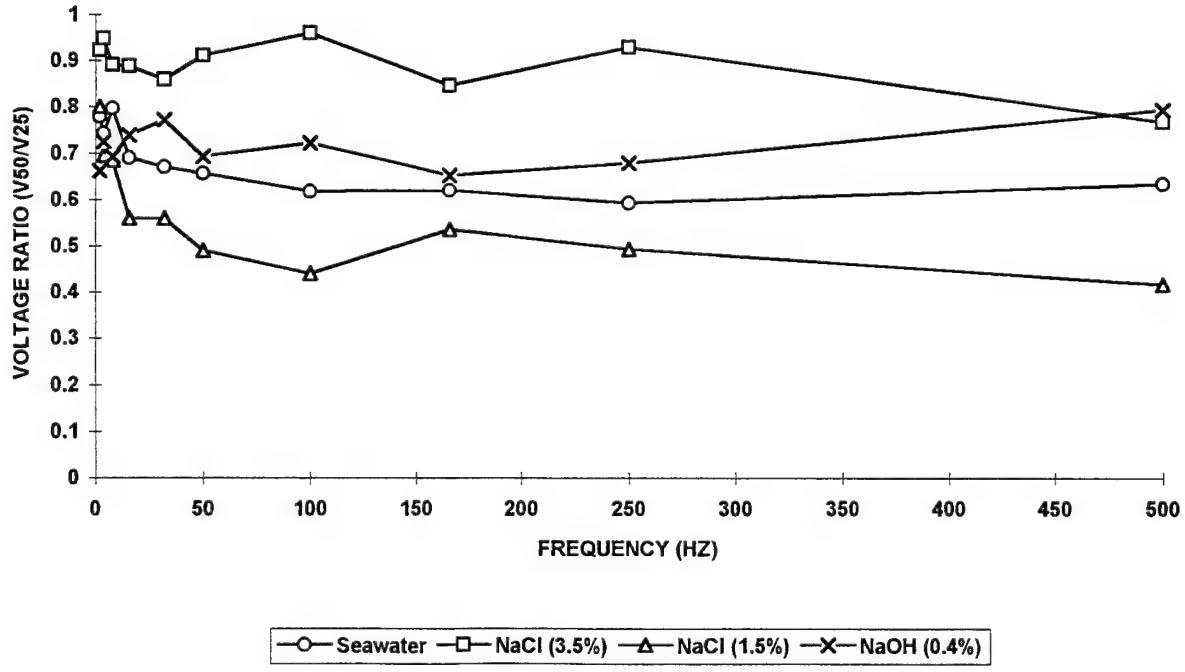

Figure 11. Ratio of Bubble-Threshold Voltages at 50-Percent Duty Cycle Relative to 25-Percent Duty Cycle (Plotted as a Function of Pulsing Frequency)

To test the logarithmic relationship between frequency and bubble-formation threshold voltage, a linear regression analysis was performed relating the log of the frequency and the log of the bubble-threshold voltage. The formula relating bubble-threshold voltage with frequency is then $\log (V_{thresh}) = a \log f + b$. Log-based coefficients, a, and intercepts, b, obtained from the logarithmic regression analysis along with the standard error in a are listed in table 3. A total of 10 frequencies were used in the logarithmic regression. The sea water test case shows the smallest relative standard error on the order of 2.25 percent. Average relative standard errors for 0.4-percent NaOH, 1.5-percent NaCl, and 3.5-percent NaCl solutions are 3.4 percent, 4.6 percent, and 5.6 percent respectively.

Table 3. Logarithmic Regression Analysis

Duty Cycle	Sea Water	0.4% NaOH	1.5% NaCl	3.5% NaCl
25%	0.379 (±0.008) +0.094	0.403 (±0.012) +0.062	0.358 (±0.010) 0.358	0.246 (±0.016) +0.062
50%	0.329 (±0.008) +0.0025	0.411 (±0.014) -0.098	0.252 (±0.016) +0.134	0.230 (±0.011) +0.039

3.2 HOT-FILM STUDIES

To determine the impact of bubble formation on the hot-film probes, a hot-film probe was situated proximal to the MHD element. The goal of the study was to determine whether the electromagnetic fields produced by the MHD element caused bubbles to form on the hot-film or whether the gas produced by the bubbly wake caused bubbles to form on the surface of the hot-film probe. A localized jet was placed to produce a flow proximal to the hot-film and was situated to test the two hypotheses. In positions 1 and 3, the jet caused the bubble stream to advect over the hot-film. In position 2, the jet was placed to deflect the bubble stream so the only influence on the hot-film would be the electromagnetic field.

Figure 12 shows the surface of the hot-film probe (position 1). There was no external flow; buoyancy was the only factor influencing the advection of the bubbles over the probe. As shown, very large bubbles accumulated on the surface of the film and appeared to cover the entire probe surface. These bubbles generally remained attached to the surface of the probe. Occasionally, an advecting bubble would "knock" one of the bubbles off, but another bubble immediately replaced it. Because the surface of the hot-film was not entirely smooth, surface-tension effects may have played a role.

A cross-flow velocity was then added. The bubbles then advected close to the probe, and an added cross-flow advected them in a direction perpendicular to the natural upward velocity attributed to buoyancy. Figure 13 shows the hot-film probe in position 1 with the added cross-flow at the lower velocity (approximately 0.5 ft/sec). As shown, the entire surface of the hot-film was covered by bubbles. Photographs were not taken for the highest cross-flow velocity (approximately 3 ft/sec) as the bubbles did not clearly show up in the photographs obtained from the video tapes. When the bubble size was analyzed directly from the video, it was observed that their size was considerably smaller than the bubbles with no jet flows. Although these bubbles were smaller, they still covered a significant portion of the surface.

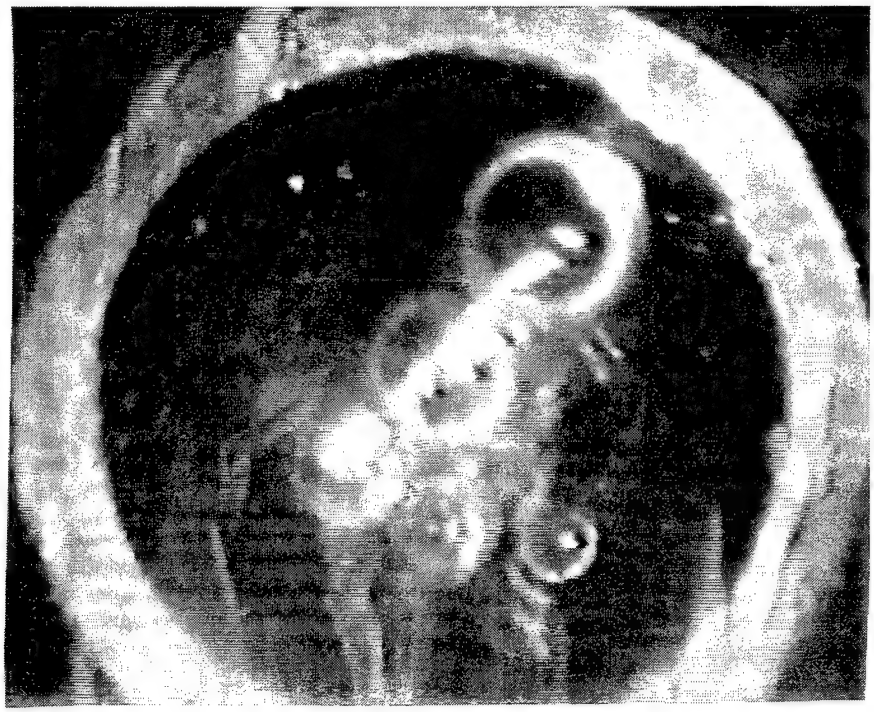

Figure 12. Surface of the Hot-Film Probe for Position 1 and No-Flow Test Case

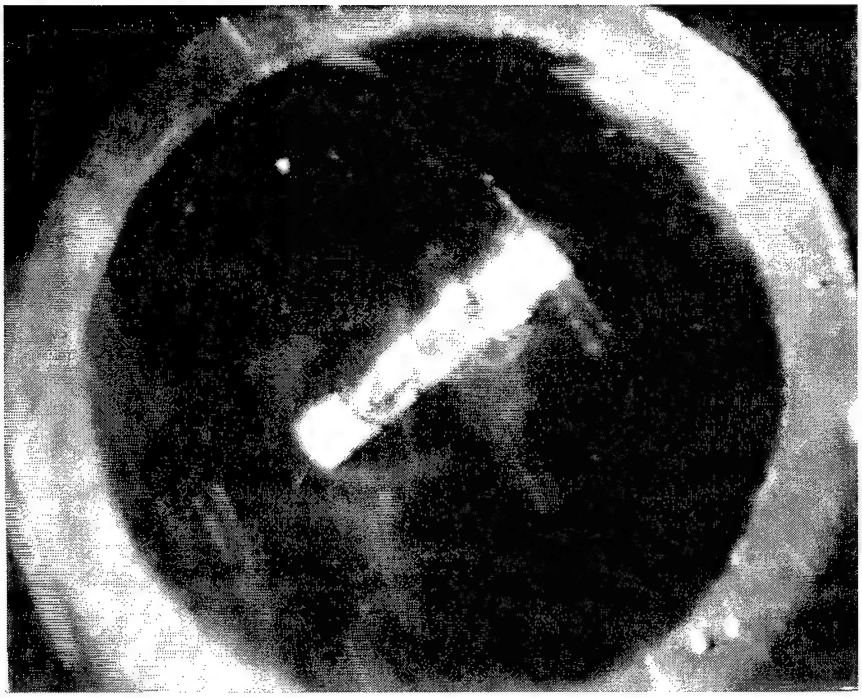

Figure 13. Surface of the Hot-Film Probe for Position 1 and Pump Setting 20

The localized jet was then placed in position 2 to deflect the bubble stream away from the hot-film probe. There was no sign of bubble formation on the surface of the hot-film. Monitored hot-film signals (using an oscilloscope) showed significant fluctuations in output voltage, suggesting the frequency response of the hot-film probes remained intact. When the localized jet was placed in position 1, significant fluctuations in bridge voltage were observed when the MHD element was turned off and no bubbles were produced. As the MHD element was turned on and bubbles began to form on the surface of the hot-film, little, if any, bridge voltage fluctuations were observed. This result suggested that the hot-film lost its frequency response.

Because it was possible that surface-tension effects were not entirely eliminated, the cross-flow jet was placed in position 3. This position resulted in the bubble stream being blown over the hot-film probe. In addition, it was found that the wake of the jet contained bubbles that were significantly smaller than those produced in position 1. Figure 14 shows the hot-film probe in position 3 with the added cross-flow at the lowest velocity. Bubbles completely covered the surface. The size of these bubbles is smaller than the size of those of position 1 and the low-speed flow case. The video was analyzed directly for the high speed. Of all test cases examined, the bubble size was the smallest and, as a percentage, the area occupied by bubbles was considerably smaller than in other test cases. Even though the surface of the film was covered by less bubbles, the actual output signal of the hot-film continued to show diminished frequency response compared with the no-bubble case.

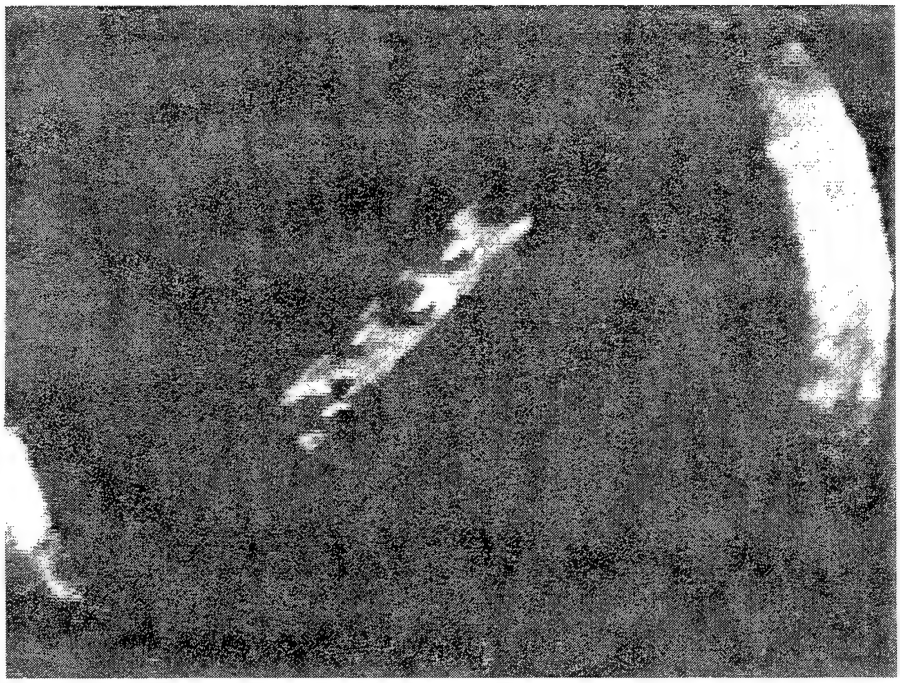

Figure 14. Surface of the Hot-Film Probe for Position 3 and Pump Setting 20

The size of bubbles that formed on the hot-film was measured directly from the video screen. The known size of the hot-film provided a reference length so the bubble size could more accurately be computed. Throughout the test, 20 bubbles were measured, for which averages were computed (see table 4). With no flow, the largest bubbles formed when the hot-film was in position 1. No bubbles formed on the hot-film in the position 2 setup (the bubble stream did not advect over the hot-film). For equivalent pump settings, bubbles that formed on the hot-film in position 1were larger than those formed in position 2.

Table 4. Computed Average Bubble Size

Pump Setting	**Bubble Size (microns)**			
	Position 1		**Position 3**	
	Average	**Range**	**Average**	**Range**
0	302	170-600	no bubbles	
20	206	100-300	100	50-150
25	131	50-250	20	10-30
30	67	40-150	10	5-15

4. DISCUSSION

The experiments conducted in this study were intended to quantify the limits of bubble production by MHD electrodes in different conducting media and the performance of hot-film anemometers in salt water MHD flows. A magnified video image was displayed on a monitor, and bubble initiation was observed for both static and pulsed current through the electrodes. Every effort was made to be consistent when judging the initiation of the bubbles. Because of the inherent subjective nature of using a visual quantifier, there was a probable 5-percent uncertainty in determining the threshold voltages. The data and subsequent observations presented in this report are intended to demonstrate specific trends and rough guidelines regarding bubble initiation and formation. Improved methods to more accurately quantify the nature and extent of bubble initiation and production can probably be made in the future.

Inorganic salts (whether NaCl, NaOH, or the many constituents of sea water) are the media that make water conductive. When NaCl is added to water, the electrostatic bond between the sodium and chlorine is broken leaving positive sodium ions and negative chlorine ions (see Hildebrand and Powell, 1952). These ions allow for a current path as the electrons leave the cathode and enter the anode thus establishing a current. Because of its chemical composition, NaCl is classified as a strong electrolyte, and the conductivity varies according to the concentration of NaCl in the water. In general, salts are highly ionic when in solution. For very dilute solutions, the constituent ions are far apart and do not influence each other. As the concentration increases, however, electrostatic attraction between the oppositely charged ions restricts the independence of individual ions and prevents the ions from exerting their full effect in terms of conducting the current. Consequently, the ions suffer an electrostatic drag effect as they move in opposite directions while conducting current. This phenomenon suggests a saturation for salt in terms of electrical conductivity and may be examined in future studies.

Bubbles are formed as electrons enter the fluid and react with hydrogen ions and chlorine ions to form their respective gases. The actual current path is established by the ions present in NaCl (or NaOH). A minimum voltage, however, is required to establish the current path. This minimum voltage arises from the aligning of the water molecules along the electric field lines. By aligning the water molecules along the electric field lines, the current is effectively canceled from the reversed polarity. The magnitude of this voltage has been estimated at 1.3 V to overcome this effect. As the voltage is increased, the electric field becomes stronger and the movement of the water and salt ions is restricted. Additional electrons enter the fluid as current is increased. Electrons enter the solution at the cathode and rupture the hydrogen bonds of the water (see Horne, 1969). Gaseous hydrogen is produced according to $H^+ + e^- = H$ followed by $2H = H_2$. Electrons leave the solution at the anode, producing the reaction $Cl^- = Cl + e^-$ followed by a combination of two chlorine atoms to form Cl_2 (see Hildebrand and Powell, 1959). Similarly, hydrogen and oxygen gases are formed as free electrons react with the OH^- chain in NaOH.

It was demonstrated that bubble threshold voltage varied logarithmically as a function of pulsing frequency. Maximum relative standard errors were below 6 percent for all the various

conducting fluids as well as the duty cycles examined. An increase in duty cycle resulted in a decreased bubble-threshold voltage. One explanation for this trend is that, for the 25-percent duty cycle, power was cut off to the electrodes for half the period, which, by definition, results in a reduction in RMS voltage by 30 percent. The ratio between the voltages for 50-percent relative and 25-percent duty cycle was expected to be 0.7. For most cases, the ratio was significantly different from 0.7 as demonstrated in figure 12. Only for sea water and the 0.4-percent NaOH solution did the ratios remain close to 0.7. For the 3.5-percent NaCl solution, the ratio was much higher (on the order of 0.9), indicating a decrease in the voltage was required to generate bubbles. Alternatively, the 1.5-percent NaCl solution showed ratios on the order of 0.55, indicating an increase in voltage was required to generate bubbles. The presence of heavy metals in the tap water altering the conductivity of the solutions was considered as an explanation. The ratios, however, were not consistently above or below 0.7 for all solutions. It is possible that the relative chemical concentrations of NaCl changed the fundamental processes as chlorine and hydrogen gases were produced.

Physically, sea water contains many constituents in addition to NaCl. Lin et al (1991) provides a listing of some of the constituent chemical components of sea water. NaCl makes up more than 90 percent of the total solids. The other solids, however, combine with water to form their components and do exist in significant quantities. After NaCl, Horne (1969) states, magnesium sulfur oxide ($MgSO_4$) occurs in the next highest concentration in sea water. While NaCl is a strong electrolyte, $MgSO_4$ is a weak one. $MgSO_4$ effectively reduces the overall conductivity of sea water and helps explain why the man-made 3.5-percent salt water was so much more conductive and bubble-producing than was the sea water.

Pulsing of the electrodes resulted in bubble formation delayed to higher voltages, which introduces unsteady effects regarding: (1) the accumulation of gas to form a bubble and (2) the variation of conductivity due to the pulsing. Finite times are required to establish the reactions to form hydrogen and chlorine gas. The gas must accumulate to form a bubble. As voltage increases, increased localized reactions occur providing a mechanism to accumulate enough gas in the form of a bubble. Pulsing delays this mechanism and allows the hydrogen gas in solution to be transported away (either from velocity of the fluid or buoyancy effects) before a gas bubble can form. Pulsing at higher frequencies delays this mechanism to higher voltages. Current results showed that as the duty cycle was decreased from 50 percent to 25 percent, bubble-threshold voltage increased. RMS voltage, however, did not completely explain this phenomenon. It is possible that the ion mobility constant and the transient in solution conductivity may have had some effect.

Others have shown that pulsing of the current can temporally alter the local conductivity of the solutions examined. Lin et al (1991) injected acid into a solution to locally increase conductivity of the sea water and thus increased the magnitude of the Lorentz force. They pulse-injected the acid, and the duration of the pulse lasted 0.3 second. They measured the solution conductivity as a function of time and noted a transient peak in the solution conductivity. Although the pulse lasted 0.3 second, the conductivity of the fluid increased to over 0.5 second even though the conducting medium was transported away. These results suggest that the present pulsed current experiments may have temporally affected the conductivity of the fluid. The medium required a finite time to establish a current path from the anode to cathode and may be

referred to as an ion mobility constant. This finite time arises from the requirement that the water and ions align themselves appropriately. As the pulsing frequency increases, the ion mobility constant may be approached, suggesting that for high enough frequencies, no current path will be established. This hypothesis may be tested in future tests.

It was clearly demonstrated that immersion of an activated hot-film probe in a wake of electrolytic bubbles resulted in bubble accumulations on the surface of the film. When this bubble accumulation occurred, the frequency response of the hot-film probe was significantly diminished. The heat-transfer coefficient of a gas is significantly less than that of liquid water; consequently, there is little heat transfer to the water because the gas bubbles act as a thermal insulator. Since the voltage is related to the heat transfer and then to the fluid velocity (via King's Law), the bubbles effectively insulate the hot-film and velocity fluctuations cannot be measured. When the bubbly wake was displaced away from the hot-film, no bubbles accumulated on the surface. This result demonstrates that the electromagnetic field produced by the MHD element has no causal effect on the bubble formation on the surface of the hot-film. Even for steady-state voltages as high as 30 V (where a great deal of bubbles were produced), no bubbles formed as long as the bubbly wake was deflected away from the hot-film. This finding has important implications in terms of possible flow measurement limitations. If the hot-film probe is placed away from a bubbly wake or if bubbles are eliminated, data from the hot-film should remain valid.

Flow velocity had a significant effect on bubble size. This flow velocity factor introduces three contributing factors to bubble formation and size: surface tension, the actual drag force on the bubbles due to the local flow velocity, and the buoyant force. The buoyant force is given simply as

$$F_b = \rho V g, \tag{1}$$

where ρ is the density of the water, V is the volume of the bubble (= $4/3\pi a^3$ where a is the bubble radius and assuming a perfect sphere) and g is the gravitational force. The drag on the sphere was computed by Stokes (see Batchelor, 1967) assuming low Reynolds number flows. The drag force is given as

$$F_d = 6\pi\mu U a \tag{2}$$

where U is the fluid velocity and μ is the coefficient of viscosity. Finally, a full derivation summarizing the effects of surface tension is too lengthy to present here. A full summary is provided by Batchelor (1967) and describes the relationship between the pressure difference across the bubble and the energy required to maintain a bubble interface. This relationship is expressed as

$$\Delta p = \gamma(1/R_1 + 1/R_2) \tag{3}$$

where γ is the surface tension coefficient, Δp is the pressure jump across the interface, and R_1 and R_2 are the principal radii of curvature. For the case where the bubble interacts with a solid surface, one of the principal radii of curvature becomes zero and, therefore,

$$\Delta p = \gamma / R. \tag{4}$$

Therefore, the size of the bubble depends on the pressure difference across the surface of the bubble. Integration over the surface of the bubble gives the actual force required to maintain the surface of the bubble. The surface tension creates a force causing it to "stick" to the solid surface. This force must be balanced by the drag force and buoyant force and governs the size of the bubble. Using the no-flow case (where only buoyancy effects are considered), bubble size is 302 microns. Therefore, the buoyant and surface tension forces should be balanced; the surface-tension force is

$$F_S = F_b = 1.16 \times 10^{-6} \text{ N}.$$

For the case in which the flow setting was 20, the fluid velocity was approximately 0.1 m/sec, and the bubble size was 206 microns. From equations (1) and (2),

$F_b = 0.358 \times 10^{-6}$ N (vertical direction), and

$F_d = 0.680 \times 10^{-6}$ N (horizontal).

Therefore, the magnitude of the surface-tension force is $F_S = 0.769 \times 10^{-6}$ N.

As a cross-flow velocity was introduced, an additional drag force on the bubble was introduced. For faster flow velocities, smaller bubbles remained on the surface of the hot-film. For the slower cross-flow velocities, very small bubbles on the order of 70 microns formed and seemed to persist. Although these bubbles were small compared with the surface of the hot-film, more formed on the surface, which resulted in a loss of frequency response. The loss of frequency response for the smaller bubbles was not, however, as great as the loss for the larger bubbles. The addition of a cross-flow velocity had greater effect on bubble size than did the presence of the buoyant force alone. It appeared that for the position-3 setup, the bubble size in the wake was initially considerably smaller than that in position 1 where the bubbles become large and are then deflected by the cross-flow. Consequently, there was considerable difference in the bubbles seen for position 1 (straight cross-flow jet) and position 3 (perpendicular jet). The bubbles seen in position 3 were considerably smaller as a result of the initially smaller bubble size. For the highest jet velocity, very small bubbles, on the order of 10 microns, formed on the surface.

There remains a question as to why bubbles form on the hot-film probe itself. If the original effect was surface tension alone, bubbles would form whether or not the probe was turned on. It was observed that bubbles formed only when the hot-film was turned on. When the hot-film was turned off, bubbles remaining on the surface were knocked off and no additional bubbles accumulated on the surface. It was shown that the electromagnetic fields produced by the MHD element had no effect on bubble formation. The only remaining effect is, therefore, the increased temperature of the hot-film itself. The ambient temperature or the conducting fluid was approximately 22°C. The operating temperature of the hot-film was approximately 65°C. The hot-film operated at a constant temperature (resistance). As a fluid flowed over the hot-film, the physical reaction of the film was to cool down. A feedback circuit provided added current to heat the film to maintain a constant 65°C temperature. Because the operating temperature of the hot-film is significantly greater than the ambient temperature of the fluid, a localized temperature gradient is formed proximal to the hot-film. It is possible that these localized temperature gradients cause the gas to come out of solution and accumulate on the surface of the hot-film. Additional tests should be conducted to confirm or deny this hypothesis.

5. CONCLUSIONS

Experiments were conducted to determine the mechanisms of bubble production by MHD electrodes and to gauge the effects of bubbles on the frequency response of hot-film probes. Closeup video photography (approximately 150x magnification) was used as visual quantifier to gauge bubble-threshold formation. These data demonstrate consistent trends in bubble formation and the responsible physical mechanisms. Four different conducting solutions were examined. Effects of bubble formation were then demonstrated as they accumulated on the surface of the hot-film probe. A jet provided a localized velocity component to advect the bubbles over the hot-film or prevent them from advecting over the probe. Bubble size and characteristics were then examined when the jet was placed in various positions and set to different velocities.

Bubble-threshold formation voltages were found to increase logarithmically with pulsing frequency for all solutions examined. Threshold voltages were found to vary according to the duty cycle. Threshold voltages were higher for 25-percent duty cycle than for the 50-percent duty cycle. Effect of RMS voltage was found to offer some, but not all, explanation for this result. Pulsing of the MHD electrodes may have produced a transient effect in terms of the conductivity of the solution. There were significant differences in bubble-formation voltage over the various solutions. A 3.5-percent salt water solution was found to produce the lowest threshold voltages. This finding is consistent with it having the greatest electrical conductivity. Sea water demonstrated consistently higher bubble-threshold voltages. Even though the total solids of sea water (3.319 percent) and the 3.5-percent saltwater were found to be close, chemical composition of the sea water was suggested to offer an explanation for the differences in bubble-threshold voltages. The 1.5-percent NaCl and 0.4-percent NaOH solutions demonstrated similar results in terms of bubble-threshold voltage probably because of the similar electrical conductivity.

Bubbles were found to form on the surface of the hot-film only when it was immersed in the bubble wake produced by the MHD electrodes. When bubbles formed on the surface, the frequency response of the hot-film probe was greatly diminished as a result of the different heat transfer coefficients between the gas bubbles and the water solution. Increases in the localized jet velocity resulted in the formation of smaller bubbles on the film surface. A balance between surface tension and drag on the bubble was reached and governed the maximum bubble size to form on the hot-film. It is important to note that bubbles were not formed on the surface when the bubbly wake was deflected away from the hot-film. This observation suggests little to no effect of the electromagnetic field produced by the MHD element on bubble formation. These results demonstrate the limitation and applicability of hot-film results when investigating effects of the application of the MHD Lorentz force on possible reduction in skin friction.

Several hypotheses about bubble production and bubble formation on the surface of the hot-film probe were discussed: (1) temporal variation of solution conductivity due to current pulsing, (2) optimal salt concentrations, (3) optimal pulsing frequencies, and (4) the effect of localized temperature gradients on bubble accumulation on a surface. More research to better characterize the mechanisms of bubble formation and accumulation on various surfaces is recommended.

6. BIBLIOGRAPHY

Batchelor, G.K.(1967), *An Introduction to Fluid Dynamics*, Cambridge University Press.

Henoch, C.W.(1992), "Analysis of the Boundary Layer Thickness Over a Flat Plate Subject to an Applied Streamwise Magnetohydrodynamic Force," NUWC-NPT Technical Memorandum 92218, Naval Undersea Warfare Center Division, Newport, RI.

Henoch, C., and J.Stace (1995), "Experimental Investigation of a Salt Water Turbulent Boundary Layer Modified by an Applied Streamwise Magnetohydrodynamic Body Force," *Physics of Fluids*, vol. 6, pp 1371-1383.

Hildebrand, J.H., and R.E. Powell (1952), *Principles of Chemistry*, Sixth Edition, Macmillan.

Horne, R.A. (1969), *Marine Chemistry*, Wiley - Interscience.

Lin, T.F., J.A. Gilbert, J.A. Nagger, and T.B. Imblum (1991), "Seawater Conductivity Enhancement by Acid Injection for the MHD Thrusters," *Proceedings of the IEEE OCEANS'91*, Honolulu, Hawaii, pp. 1629-1635.

Meng, J.C.S. (1995), "Wall Layer Microturbulence Phenomenology and a Markov Probability Model for Active Electromagnetic Control of Turbulent Boundary Layers in an Electrically Conducting Medium," NUWC-NPT Technical Report 10,434, Naval Undersea Warfare Center Division, Newport, RI.

Nosenchuck, D., and G. Brown (1995), "The Direct Control of Wall Shear Stress in a Turbulent Boundary Layer," submitted to *Physical Review Letters.*

Nosenchuck, D. (1995), Private Communications.

INITIAL DISTRIBUTION LIST

Addressee	No. of Copies
Office of Naval Research (Code 333 (S. Lekoudis, L. Purtell, J. Fein, E.Rood))	4
Center for Naval Analyses	1
Defense Technical Information Center	2
Advanced Research Projects Agency (G. Jones)	1